Luminescent Enhancement of Na^+ and Sm^{3+} Co-doping Reddish Orange $SrCa_3Si_2O_8$ Phosphors

Fengjun Chun, Binbin Zhang, Wen Li, Honggang Liu, Wen Deng, Xiang Chu, Hanan Osman, Haitao Zhang & Weiqing Yang

Journal of Electronic Materials

ISSN 0361-5235
Volume 47
Number 4

Journal of Elec Materi (2018)
47:2386-2393
DOI 10.1007/s11664-017-6030-7

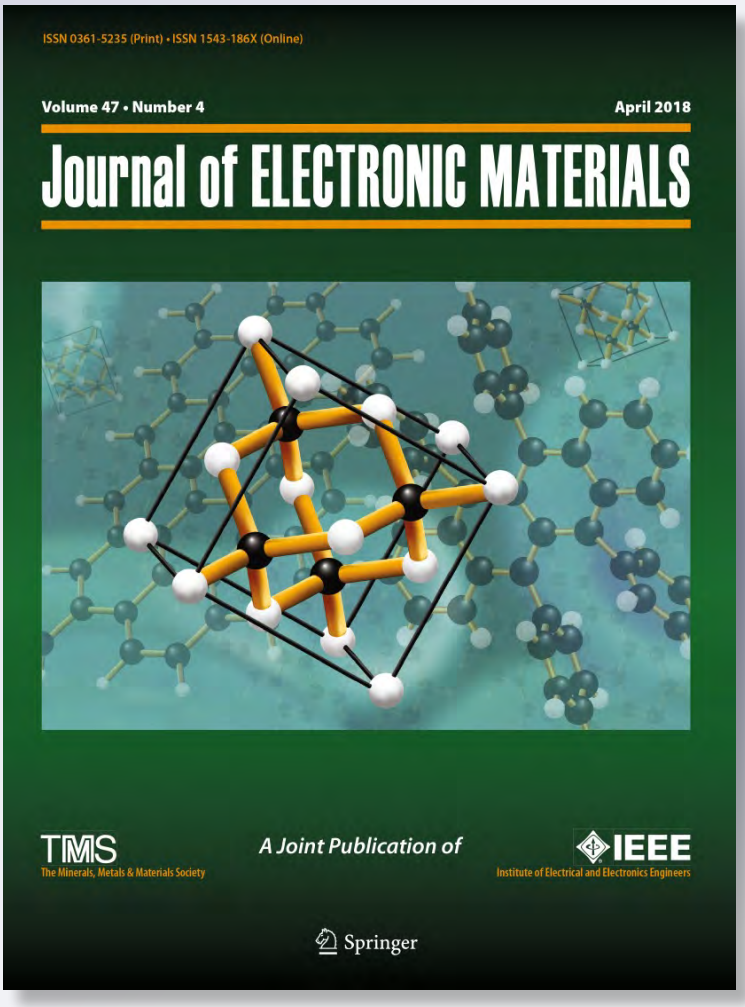

Springer

Journal of ELECTRONIC MATERIALS, Vol. 47, No. 4, 2018
https://doi.org/10.1007/s11664-017-6030-7

Luminescent Enhancement of Na^+ and Sm^{3+} Co-doping Reddish Orange $SrCa_3Si_2O_8$ Phosphors

FENGJUN CHUN,[1] BINBIN ZHANG,[1] WEN LI,[1] HONGGANG LIU,[2] WEN DENG,[1] XIANG CHU,[1] HANAN OSMAN,[1] HAITAO ZHANG,[1] and WEIQING YANG [1,3]

1.—Key Laboratory of Advanced Technologies of Materials (Ministry of Education), School of Materials Science and Engineering, Southwest Jiaotong University, Chengdu 610031, China. 2.—Department of Materials Science, Sichuan University, Chengdu 610064, China. 3.—e-mail: wqyang@swjtu.edu.cn

Reddish orange $SrCa_3Si_2O_8$ phosphors, prepared by the facile solid state reaction method, are a luminescent enhancement of Na^+ and Sm^{3+} co-doping luminescent material. Na^+ was designed to compensate the charge imbalance of Sm^{3+} ion substituting for the Sr^{2+} ion of orthorhombic $SrCa_3Si_2O_8$ crystals. The results suggest that Na^+ can effectively enhance the luminescent intensity of the reddish orange light peaked at about 562 nm ($^4G_{5/2} \rightarrow {}^6H_{5/2}$), 600 nm ($^4G_{5/2} \rightarrow {}^6H_{7/2}$) and 645 nm ($^4G_{5/2} \rightarrow {}^6H_{9/2}$) excited by the near ultraviolet excited light 404 nm ($^4L_{13/2} \rightarrow {}^6H_{5/2}$). The energy transfer has been further verified by the florescence lifetime. Additionally, the luminescent lifetime τ of as-grown phosphors was separated into two parts, a rapid lifetime and a slow lifetime. The average lifetime results ranged from 2.098 to 1.329 ms which were influenced by the concentration of Sm^{3+} doping. The systematic researches of as-grown phosphors have clearly suggested a potential application for white-light-emitting diodes (w-LEDs).

Key words: White-light-emitting diodes, rare earths, luminescent spectra, $SrCa_3Si_2O_8$:Sm^{3+}, Na^+

INTRODUCTION

White-light-emitting diodes (w-LEDs) have attracted considerable interest in recent years due to their superior features such as high color rendering index (CRI), high luminosity efficiency, and low energy consumption, which is evidenced to be the next-generation light source for solid-state lighting.[1–6] Currently, major commercial w-LEDs contain two prototypes. One was designed by combining yellow- and red-emitting phosphors with GaN-based blue light-emitting diode (LED) chips.[7–9] The other prototype w-LEDs device was fabricated by coating blue-, green- and red-emitting phosphors onto GaAlN-based ultraviolet (UV) LEDs chips.[10,11] Such a combination offers high luminescence efficiency, whereas it causes a poor color rendering index (< 80) due to the red-emitting phosphors with relatively low luminescence efficiency.[12] In order to address the limited luminescence efficiency of red-emitting phosphors, researchers have exploited various rare earth ions doped red phosphors, such as CaS:Eu^{2+},[13] $SrMoO_4$ ($BaMoO_4$):Eu^{3+},[7] $Ba_3Bi(PO_4)_3$:Sm^{3+},[14] CaTiO3 ($SrTiO_3$, $BaTiO_3$):Pr^{3+}.[15] The reported Eu^{3+}-doping red phosphors with enhanced color rendering capabilities can effectively be excited by GaN-based (about 460 nm) chips other than GaAlN-based near UV chips, whereas the near UV-based (about 400 nm) w-LEDs are evaluated as a more effective packaging model to improve CRI of w-LEDs.[8,9] It is noteworthy that Pr^{3+} and Sm^{3+} doping phosphors can be excited by near UV light,[16–18] and the Sm^{3+} ion is consistently regarded as considerable doping ions for the orange-red luminescent materials due to its intense $^4G_{5/2} \rightarrow {}^6H_J$ emission range from 550 nm to 670 nm.[19]

(Received July 24, 2017; accepted December 12, 2017; published online January 19, 2018)

Recently, various tungstate, molybdate, oxybromide, silicate and phosphates phosphors, doped with Sm^{3+}, have been reported to be extensively used in *w*-LEDs.[20–22] Besides, silicates have been hailed as remarkable host crystals owing to their outstanding thermal, chemical, and mechanical stability.[23–26] Eu^{3+} and Pr^{3+} doped red silicates phosphors have been widely reported to date,[23–26] while Sm^{3+}-doping silicates phosphors have rarely been reported previously, because the charge mismatch and charge defect may occur when Sm^{3+} ions are substituted to be adaptable to compensate for the charge imbalance imposed by different cation substitution.[27,28] Hence, it is necessary to utilize a co-doping method to boost the luminescence efficiency of red-emitting phosphors.

Herein, we present Na^+ and Sm^{3+} co-doping reddish orange $Sr_{1-x-y}Ca_3Si_2O_8:Sm_x^{3+}$, Na_y^+ phosphors by the simple and effective solid state reaction. The effects of the different Sm^{3+} and Na^+ concentrations on the luminescence intensity and lifetime have been discussed in detail. Our study also proved that the luminescence properties of $SrCa_3Si_2O_8:Sm^{3+}$ with Na^+ doping can effectively enhance the luminescent intensity of as-grown phosphors. It evidently demonstrates a promising reddish orange phosphor for *w*-LEDs.

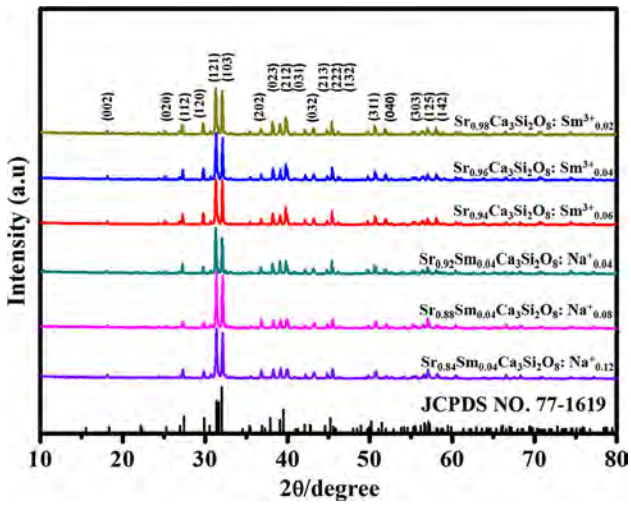

Fig. 1. XRD patterns of $Sr_{1-x}Ca_3Si_2O_8:Sm_x^{3+}$ (x = 0.02, 0.04 and 0.06) and $Sr_{0.96-y}Sm_{0.04}Ca_3Si_2O_8:Na_y^+$ (y = 0.04, 0.08 and 0.12) phosphors.

MATERIALS AND METHODS

A series of $Sr_{1-x-y}Ca_3Si_2O_8:Sm_x^{3+}$, Na_y^+ reddish orange phosphors were successfully prepared by the conventional solid state reaction method. Appropriate amounts of $SrCO_3$ (99.5%), $CaCO_3$ (99.5%), Sm_2O_3 (99.99%), SiO_2 (99.9%) and Na_2CO_3 (99.5%) were selected as the starting raw materials and were mixed homogeneously in an agate mortar. The molar composition was Sr^{2+}:Ca^{2+}:Si^{4+}:Sm^{3+}:-Na^+ = 1_x_y:3:2:x:y (x = 0 mol.%, 1 mol.%, 2 mol.%, 3 mol.%, 4 mol.%, 5 mol.%, 6 mol.%, y = 0 mol.%, 2 mol.%, 4 mol.%, 6 mol.%, 8 mol.%, 10 mol.%, 12 mol.%). The mixed powders were put into a corundum crucible and firstly calcined at 600°C for 3 h, and then calcined at 1500°C for 5 h in

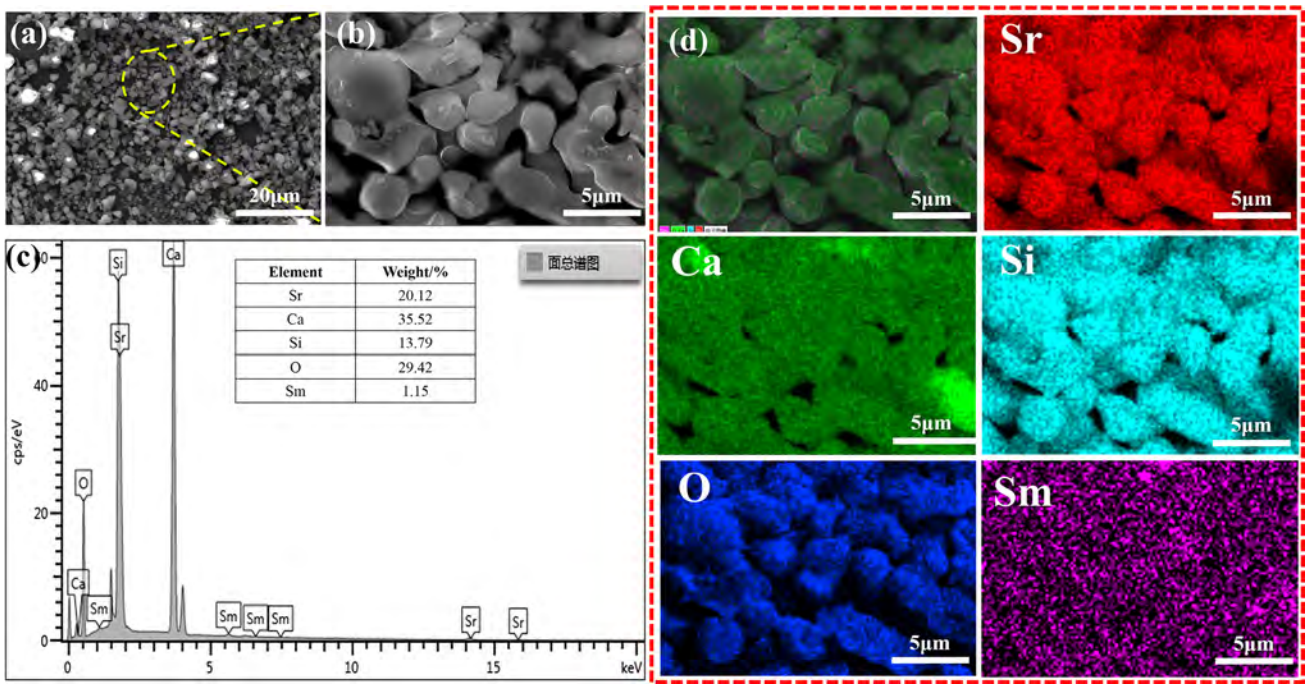

Fig. 2. The surface microscopic morphology of $Sr_{0.96}Ca_3Si_2O_8:Sm_{0.04}^{3+}$ phosphors: (a) SEM, (b) enlarged SEM, and (c, d) EDS images.

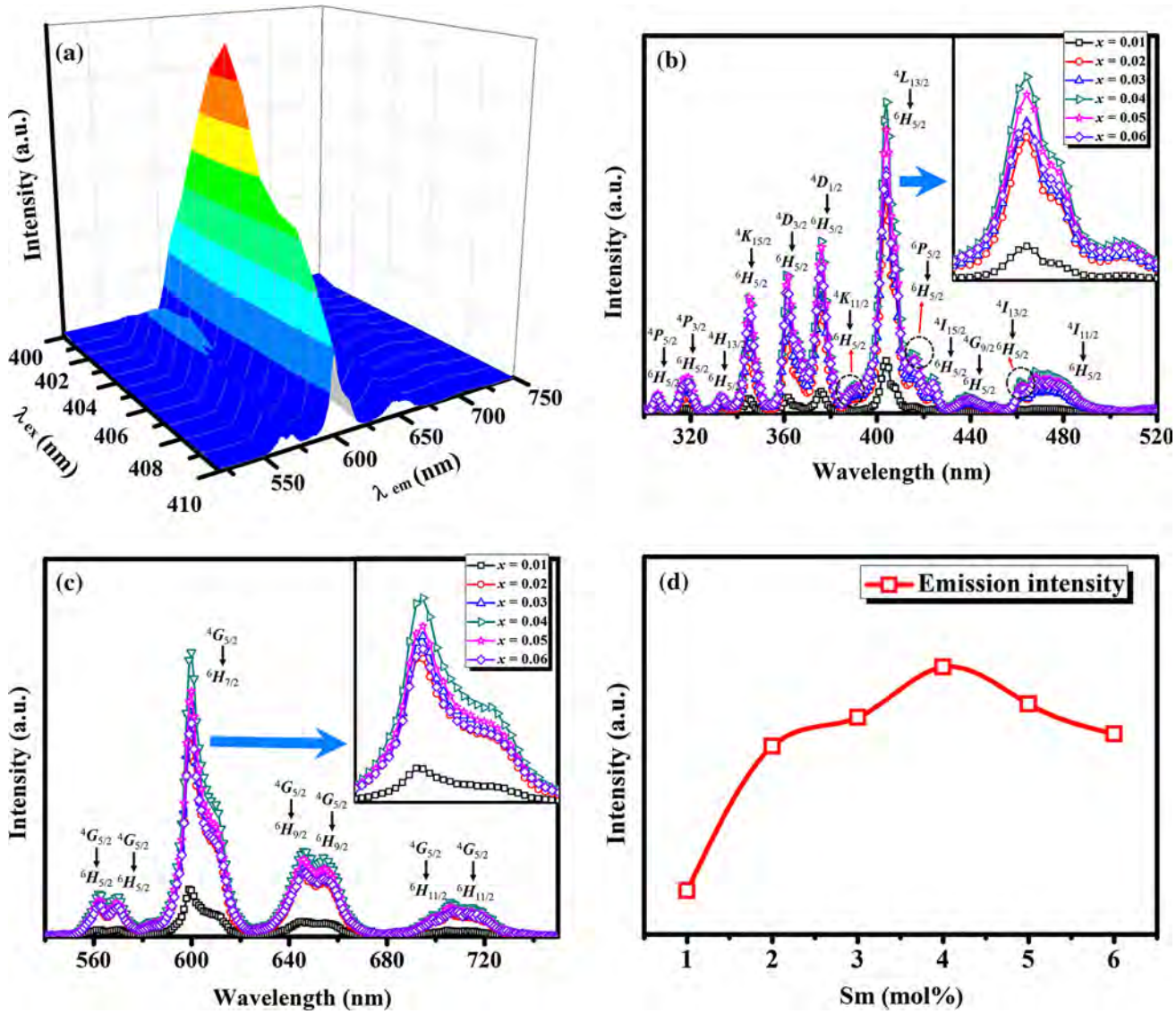

Fig. 3. (a) Emission spectra and intensities of $Sr_{0.96}Ca_3Si_2O_8:Sm^{3+}_{0.04}$ with the various excitation wavelengths ranging from 400 nm to 410 nm. (b, c) Excitation (b) and emission (c) spectra of $Sr_{1-x}Ca_3Si_2O_8:Sm^{3+}_x$ (x = 0.01–0.06) phosphors with emission wavelength 600 nm and excitation wavelength 404 nm; (d) emission intensities of $Sr_{1-x}Ca_3Si_2O_8:Sm^{3+}_x$ with the various Sm^{3+} doping concentrations.

air. The final phosphors were obtained after grinding.

The phase composition of $Sr_{1-x-y}Ca_3Si_2O_8:Sm^{3+}_x$, Na^+_y phosphors were identified by the X'Pert Pro MPD (Holland) x-ray diffraction meter with Cu $K_{\alpha 1}$ radiation (λ = 0.154 nm). The morphology and element compositions were recorded using scanning electron microscopy (SEM, S4800) and energy-dispersive x-ray spectroscopy (EDS, S4800), respectively. Luminescence spectra and lifetimes were investigated at room temperature using a FLS980 (Edinburgh Instruments) spectrometer with a 450 W Xenon lamp and a 60 W microsecond pulsed xenon flash lamp, respectively.

RESULTS AND DISCUSSION

The crystallinity characterizations of $Sr_{1-x}Ca_3Si_2O_8:Sm^{3+}_x$ (x = 2 mol.%, 4 mol.%, 6 mol.%) and $Sr_{0.96-y}Sm_{0.04}Ca_3Si_2O_8:Na^+_y$ (y = 4 mol.%, 8 mol.%, 12 mol.%) phosphors with arbitrary composition were determined by x-ray powder diffraction, as shown in Fig. 1. The diffraction pattern for all samples are similar and no extra peaks are detected, and the diffraction peaks are assigned to crystalline $SrCa_3Si_2O_8$ (JCPDS No. 77-1619) with the tunable Sm^{3+} and Na^+ contents.[26,29] This result reveals the crystalline structure of $SrCa_3Si_2O_8$ cannot be affected by co-doping Sm^{3+} and Na^+ ions, which is ascribed to the perfect incorporation of Na^+ and Sm^{3+} into the host lattices. No other impurity phases can be detected,

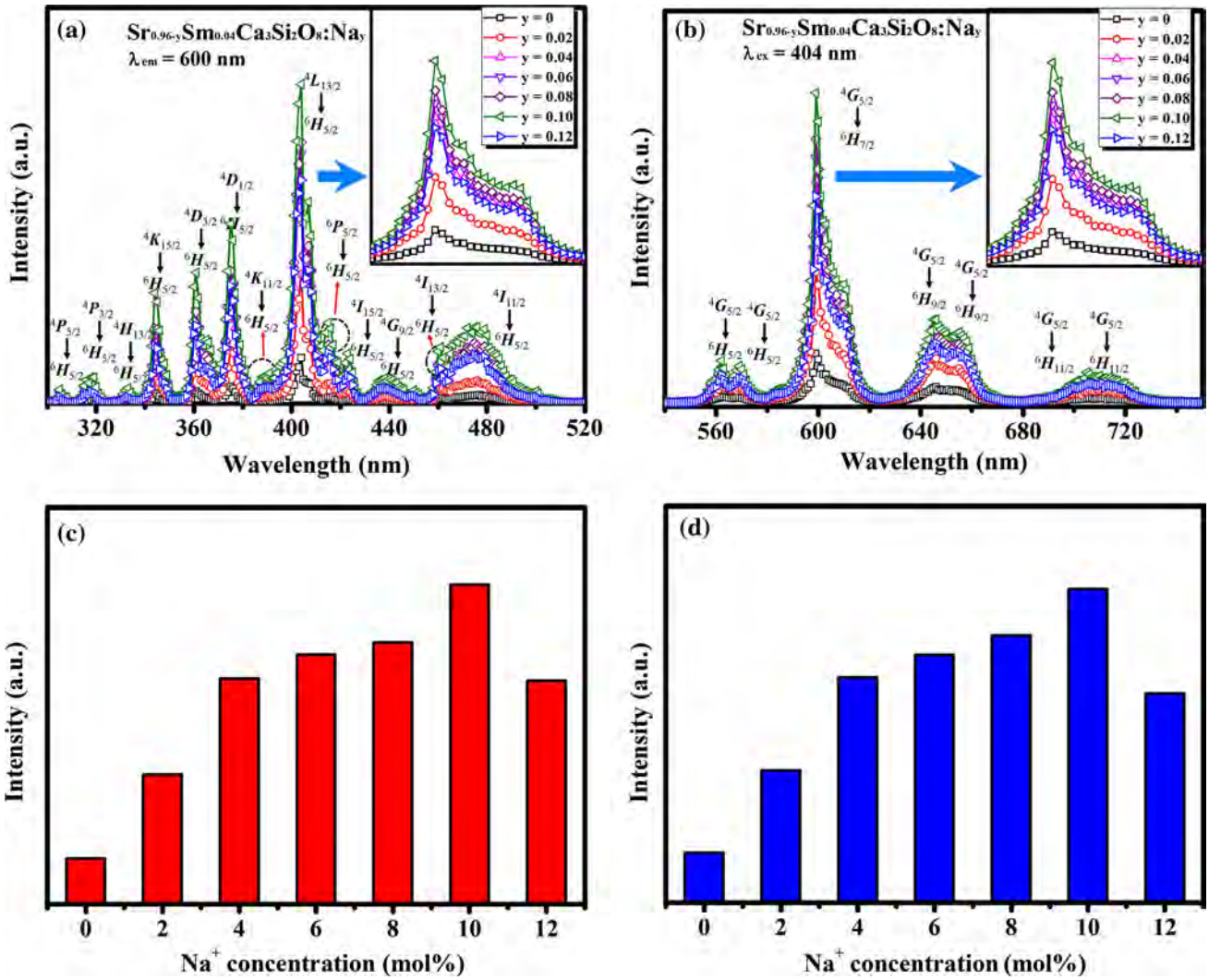

Fig. 4. (a, b) Excitation (a) and emission (b) spectra of $Sr_{0.96-y}Sm_{0.04}Ca_3Si_2O_8:Na_y^+$ (y = 0.02–0.12) phosphors; (c, d) excitation (c) and emission (d) intensities of $Sr_{0.96-y}Sm_{0.04}Ca_3Si_2O_8:Na_y^+$ (y = 0.02–0.12) phosphors.

implying that almost pure $Sr_{1-x-y}Ca_3Si_2O_8:Sm_x^{3+}$, Na_y^+ was obtained.

The morphology and particle size commonly affect the luminous and heat dissipation efficiency of phosphors. SEM images (Fig. 2a and b) clearly present the irregular $Sr_{0.94}Ca_3Si_2O_8:Sm_{0.04}^{3+}$ crystals with the diameter of about 2–6 μm, the particle size is conducive to the encapsulation of LEDs. Moreover, the element distribution and the nominal stoichiometry were explored by using the SEM-EDS mapping analyses. According to the EDS spectra (Fig. 2c), the Sr, Ca, Si, O and Sm elements can be detected in the phosphors, and the mass ratio of different elements, M_{Sr}:M_{Ca}:M_{Si}:M_O:M_{Sm} (0.68:0.93:0.44:1:0.04), is in close agreement with the stoichiometry of $Sr_{0.96}Ca_3Si_2O_8:Sm_{0.04}^{3+}$, (0.68:1.21:0.46:1:0.04)). Figure 2d also illustrates Sm^{3+}-doping ions are uniformly distributed in the $Sr_{0.96}Ca_3Si_2O_8:Sm_{0.04}^{3+}$ phosphors, these results suggest that that high quality phosphors with uniform rare earth ion doping can be anticipated through the facile solid state reaction.

Figure 3 obviously demonstrates the fluorescent properties of as-grown $Sr_{1-x}Ca_3Si_2O_8:Sm_x^{3+}$ (x = 0.01–0.06) phosphors annealed at 1500°C. The emission spectra and intensities of $SrCa_3Si_2O_8:Sm^{3+}$ with the various excitation wavelengths ranging from 400 nm to 410 nm is clearly demonstrated in Fig. 3a, which indicates that 404 nm is the optimal excitation wavelength. As shown in Fig. 3b, the excitation spectra for 600 nm emission has a series of peaks located at 306 nm, 318 nm, 334 nm, 345 nm, 362 nm, 376 nm, 391 nm, 404 nm, 416 nm, 424 nm, 439 nm, 462 nm, and 474 nm, and these peaks can be attributed to the $^4P_{5/2} \rightarrow {}^6H_{5/2}$ (306 nm), $^4P_{3/2} \rightarrow {}^6H_{5/2}$ (318 nm), $^4H_{13/2} \rightarrow {}^6H_{5/2}$ (334 nm), $^4K_{15/2} \rightarrow {}^6H_{5/2}$ (345 nm), $^4D_{3/2} \rightarrow {}^6H_{5/2}$ (362 nm), $^4D_{1/2} \rightarrow {}^6H_{5/2}$ (376 nm), $^4K_{11/2} \rightarrow {}^6H_{5/2}$ (391 nm), $^4L_{13/2} \rightarrow {}^6H_{5/2}$ (404 nm), $^6P_{5/2} \rightarrow {}^6H_{5/2}$

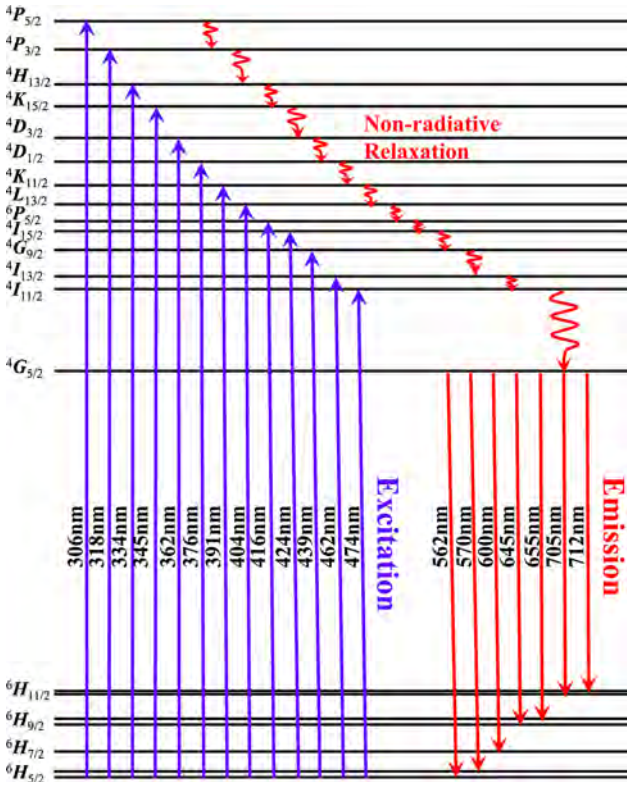

Fig. 5. The diagram of the luminescence mechanism of Sm^{3+} and Na^{+} co-doped $SrCa_3Si_2O_8$ phosphors for white LEDs.

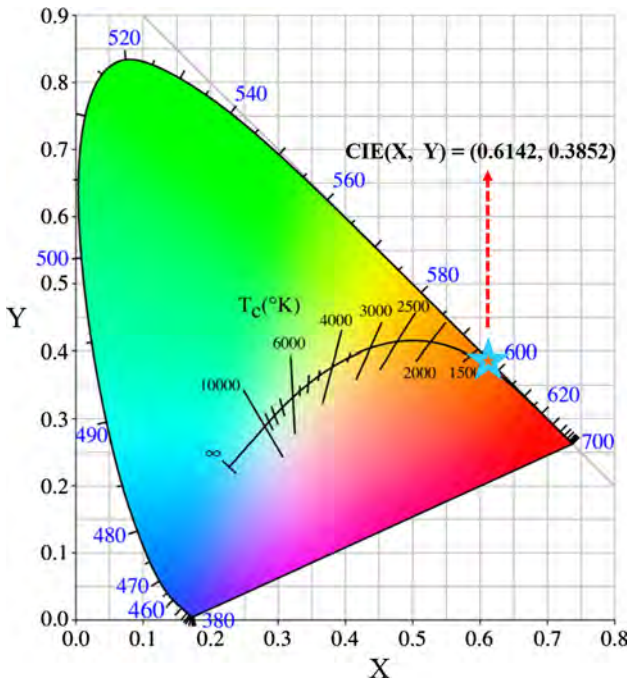

Fig. 6. The chromaticity diagram of $Sr_{0.96}Sm_{0.04}Ca_3Si_2O_8:Na^{+}_{0.1}$ phosphors.

(416 nm), $^4I_{15/2} \rightarrow {}^6H_{5/2}$ (424 nm), $^4G_{9/2} \rightarrow {}^6H_{5/2}$ (439 nm), $^4I_{13/2} \rightarrow {}^6H_{5/2}$ (462 nm) and $^4I_{11/2} \rightarrow {}^6H_{5/2}$ (474 nm) transitions of Sm^{3+} ions, respectively.[30–35] The excitation spectra evidently reveal that $SrCa_3Si_2O_8:Sm^{3+}$ can be effectively excited by near-UV and blue light LED chips. Under 404 nm excitation, the characteristic emission peaks of $SrCa_3Si_2O_8:Sm^{3+}$ were observed at 562 nm, 570 nm, 600 nm, 645 nm, 655 nm, 705 nm, and 712 nm, as illustrated in Fig. 3c. Among these peaks, the strongest peak at 600 nm corresponds to the $^4G_{5/2} \rightarrow {}^6H_{7/2}$ transitions of Sm^{3+}. The other five peaks should be ascribed to the transition of $^4G_{5/2} \rightarrow {}^6H_{5/2}$ (562 nm) $^4G_{5/2} \rightarrow {}^6H_{5/2}$ (570 nm), $^4G_{5/2} \rightarrow {}^6H_{9/2}$ (645 nm), $^4G_{5/2} \rightarrow {}^6H_{9/2}$ (655 nm), $^4G_{5/2} \rightarrow {}^6H_{11/2}$ (705 nm), and $^4G_{5/2} \rightarrow {}^6H_{11/2}$ (712 nm). Figure 3d gives the comparison of the emission intensity for $SrCa_3Si_2O_8:Sm^{3+}$ phosphors with a series of Sm^{3+} doping concentrations. The emission intensity gradually increases with increasing Sm^{3+} concentration, and reaches a maximum value at 4 mol.%. After that, the concentration quenching occurs when the concentration of Sm^{3+} increases continuously. The quenching can be attributed to the increased odds of non-radiative energy transfer from one Sm^{3+} to another. The non-radiativity is associated with the ion-ion interaction, which is provoked by the shorting distance between the nearest Sm^{3+}, the cross-relaxation processes: $^4G_{5/2} + {}^6H_{5/2} \rightarrow 2(^6F_{9/2})$ may be the major concerns for the non-radiative energy transfer from Sm^{3+} to Sm^{3+}.[36,37]

As we know, the charge imbalance, ascribed to the substitution of trivalent Sm^{3+} for divalent Sr^{2+} in $SrCa_3Si_2O_8$ phosphors, will result in a dramatic reduction of the luminescence intensity.[25] The effect is probably related to the increased concentration of oxygen vacancies that are needed for the charge compensation in the lattice. The charge generated by Sm^{3+} substitution for Sr^{2+}can be neutralized by incorporating alkali metal ions, such as Na^{+}, Li^{+}, K^{+}.[38,39] In this paper, the Na^{+} ion in Na_2CO_3 was applied to compensate for this charge imbalance ($2Sr^{2+} \rightarrow Sm^{3+} + Na^{+}$). The fluorescence spectra of $Sr_{0.96}Sm_{0.04}Ca_3Si_2O_8$ with the various Na^{+} doping concentrations ranging from 2 mol.% to 12 mol.% are demonstrated in Fig. 4a and b. It is obviously shown that the spectra of $Sr_{0.96}Sm_{0.04}Ca_3Si_2O_8:Na^{+}$ are similar to that of the as-prepared $SrCa_3Si_2O_8:Sm^{3+}$ phosphors without a charge compensator. As shown in Fig. 4c and d, the luminescence properties of $Sr_{0.96}Sm_{0.04}Ca_3Si_2O_8$ are remarkably modified by the Na^{+} doping. The luminescence intensity initially increases with increasing the amount of Na^{+}, and then decreases gradually with a further increase of Na^{+}. It reveals that Na^{+} can effectively enhance the luminescence intensity of $Sr_{0.96}Sm_{0.04}Ca_3Si_2O_8$ as a charge compensator, and the optimal Na^{+} doping concentration should be about 10 mol.%. The fluorescence emission intensity of $Sr_{0.96}Sm_{0.04}Ca_3Si_2O_8$ phosphors increased to 6.3 times after co-doping with 10 mol.% Na^{+}. Thus, excessive Na^{+} act as a charge compensator that is a necessary condition for enhancing the fluorescence

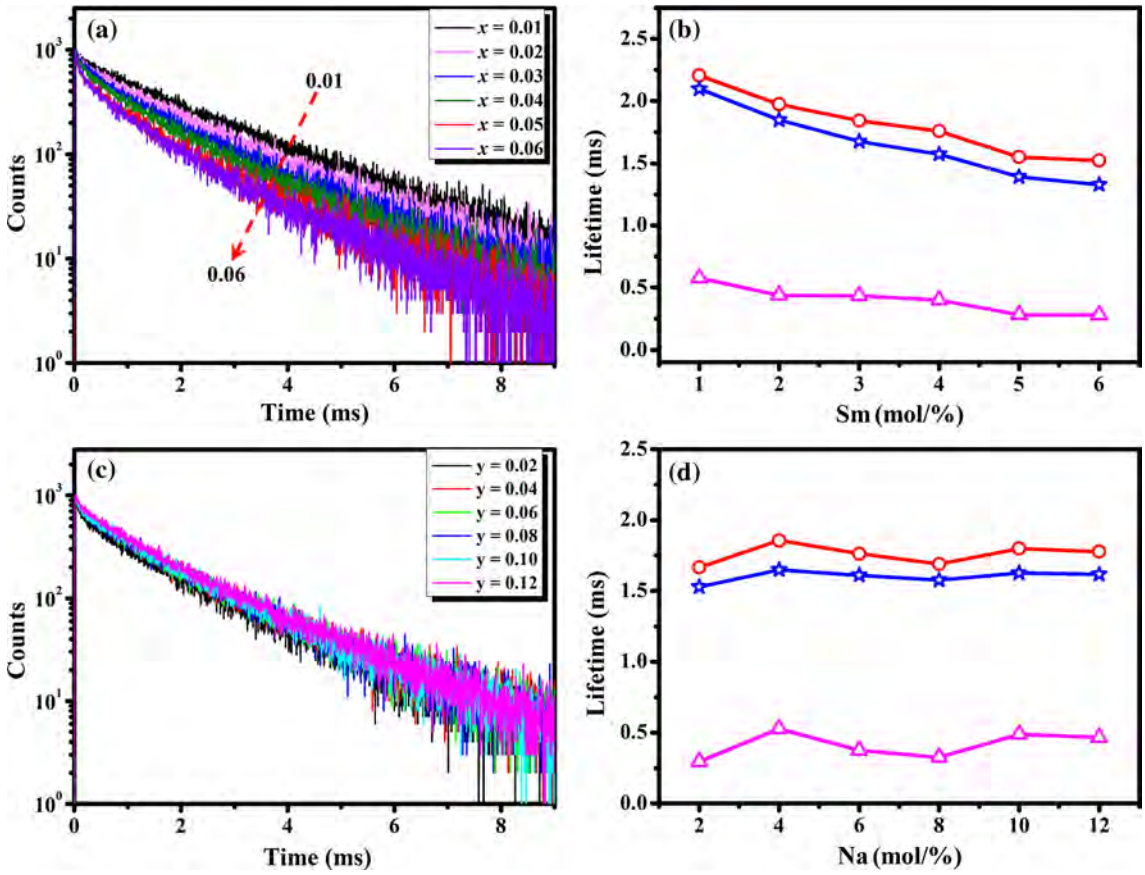

Fig. 7. (a, b) Photoluminescence decay traces of $Sr_{1-x}Ca_3Si_2O_8:Sm_x^{3+}$ (x = 0.01–0.06) phosphors with excitation wavelength 404 nm and emission wavelength 600 nm; (c, d) photoluminescence decay traces of $Sr_{0.96-y}Sm_{0.04}Ca_3Si_2O_8:Na_y^+$ (y = 0.02–0.12) phosphors with excitation wavelength 404 nm and emission wavelength 600 nm.

intensity. For the more explicit presentation of the above spectra, these transition spectra were sketched in detail in Fig. 5.[30–34]

The chromaticity color coordinates are an important index to evaluate phosphor performance. Figure 6 shows the Commission International de L'Eclairage (CIE) chromaticity diagram of $Sr_{0.96}Sm_{0.04}Ca_3Si_2O_8:Na_{0.1}^+$ phosphors upon 404 nm excitation, and the coordinates are (X, Y) = (0.6142, 0.3752). Thus, Sm^{3+} and Na^+ co-doped $SrCa_3Si_2O_8$ phosphors have potential values applied to w-LEDs.

The luminescence decay curves of $SrCa_3Si_2O_8$: Sm^{3+}, Na^+ were measured at room temperature with excitation wavelength 404 nm and emission wavelength 600 nm, as shown in Fig. 7, which can be expressed as the following equation[35]:

$$I(t) = A_1 e^{-t/\tau_1} + A_2 e^{-t/\tau_2}, \quad (1)$$

where $I(t)$ is the luminescence intensity, A_1 and A_2 are constants, t is the time; τ_1 and τ_2 are rapid and slow lifetimes, which can be fitted by the double exponential function. The average decay times (τ^*) of the $^4G_{5/2} \rightarrow {}^6H_{7/2}$ transition can be defined by the equation as follows:

$$\tau^* = (A_1\tau_1^2 + A_2\tau_2^2)/(A_1\tau_1 + A_2\tau_2). \quad (2)$$

The values of A_1, τ_1, A_2, τ_2, τ^* and x^2can be obtained in Tables I and II.

The decay curves of $^4G_{5/2} \rightarrow {}^6H_{7/2}$ transition with the various Sm^{3+} doping concentrations are clearly displayed in Fig. 7a. As shown in Fig. 7b, the calculated rapid lifetimes and slow lifetimes are decreasing with the elevation of Sm^{3+} doping concentration. The average lifetime of the $^4G_{5/2}$ is significantly reduced from 2.098 ms to 1.329 ms with the increase of Sm^{3+} ion concentration, it can be explained by a concentration quenching effect as mentioned above. As the Sm^{3+} doping concentration increases, the increased interaction or energy transfer migration among Sm^{3+} ions will result in the enhanced provability of non-radiative rate and the reduced lifetimes. Furthermore, the luminescence decay curves of $Sr_{0.96}Sm_{0.04}Ca_3Si_2O_8$ with the various Na^+ doping concentrations are demonstrated in Fig. 7c.

As illustrated in Fig. 7d, it is interesting that there was no significant change of the luminescent

Table I. Decay lifetime of $Sr_{1-x}Ca_3Si_2O_8:Sm_x^{3+}$ (x = 0.01–0.06) phosphors excited at 404 nm with the emission monitored at 600 nm

Sample	τ_1	A_1	τ_2	A_2	τ_* (μs)	x^2
x = 0.01	578.52	185.36	2204.63	691.56	2097.78	1.62
x = 0.02	437.49	246.83	1974.48	613.69	1848.71	1.69
x = 0.03	433.62	301.72	1842.72	532.92	1677.06	1.72
x = 0.04	401.48	325.59	1758.19	475.13	1574.62	1.66
x = 0.05	274.01	327.67	1543.52	427.75	1391.54	1.68
x = 0.06	279.93	392.32	1522.33	392.34	1329.37	1.71

Table II. Decay lifetime of $Sr_{0.96}Sm_{0.04}Ca_3Si_2O_8:Na_y^+$ (y = 0.02–0.12) phosphors excited at 404 nm with the emission monitored at 600 nm

Sample	τ_1	A_1	τ_2	A_2	τ_* (μs)	x^2
y = 0.02	296.34	302.56	1665.19	489.33	1529.50	1.62
y = 0.04	528.75	322.91	1855.74	500.18	1649.57	1.66
y = 0.06	376.49	313.56	1762.52	541.06	1609.84	1.60
y = 0.08	326.65	270.64	1690.84	576.14	1577.34	1.61
y = 0.10	489.02	296.29	1799.57	528.87	1626.42	1.69
y = 0.12	466.24	308.93	1777.75	582.24	1617.54	1.58

lifetimes with the changing Na^+ concentration. This Na^+ ion, as a charge compensator, is very difficult to change radiative transition mode during the energy transfer process, and it has no obvious impact on the transfer speed between ground state and excitation state.[40] In addition, there is a competition between the offset of charge imbalance and the generation of crystal lattice distortion. On the one hand, Na^+ ions as a charge compensator were employed to neutralize the charge and decrease the non-radiative transition chance. The decreased non-radiative transition chance is beneficial to the increase of lifetimes. On the other hand, ascribing to the ionic radii difference between Sr^{2+} (0.118 Å) and Na^+ (0.102 Å), the crystal lattice distortion and effects will be generated when Sm^{3+} and Na^+ ions substitute for Sr^{2+} ions.[41] This crystal lattice distortion may lead to some non-radiative transition and decrease the lifetimes.[42,43] Therefore, it is reasonable that the Na^+ doping can improve the fluorescence intensity but have a no significant influence on fluorescence lifetimes.

CONCLUSIONS

In summary, a reddish orange Na^+ and Sm^{3+} co-doping $SrCa_3Si_2O_8$ phosphor was successfully synthesized by the conventional solid state reaction method. The as-prepared phosphors can be effectively excited with a near UV light (404 nm) and exhibit orange-red fluorescence emission peaking at 562 nm, 600 nm, and 645 nm. The composition-dependent luminescence behaviors of Sm^{3+} and Na^+ co-doping $SrCa_3Si_2O_8$ phosphors were investigated, fluorescence quenching occurs when the concentration of Sm^{3+} is above 4 mol.%, as ascribing to a non-radiative energy transfer between Sm^{3+}. Furthermore, the emission intensity of $SrCa_3Si_2O_8$ phosphors can be dramatically enhanced to 6.3 times when the optimum concentration of the Na^+ charge compensator was determined to be about 10 mol.%. This evidently reveals that Na^+ and Sm^{3+} co-doping $SrCa_3Si_2O_8$ phosphors will facilitate the fabrication of w-LEDs as red phosphors and this co-doping method would be applicable to various rare earth elements doped phosphors.

ACKNOWLEDGEMENTS

This work is supported by the National Natural Science Foundation of China (Nos. 51202023 and 11028409), The Scientific and Technological Projects for Distinguished Young scholars of Sichuan Province (No. 2015JQ0013), and the Fundamental Research Funds for the Central Universities of China (A0920502051408-10 and ZYGX2009Z0001).

REFERENCES

1. C. Pan, L. Dong, G. Zhu, S. Niu, R. Yu, Q. Yang, Y. Liu, and Z.L. Wang, *Nat. Photonics* 7, 752 (2013).
2. R.R. Bao, C.F. Wang, L. Dong, R.M. Yu, K. Zhao, Z.L. Wang, and C.F. Pan, *Adv. Funct. Mater.* 25, 2884 (2015).
3. W.Q. Yang, Z.L. Liu, J. Chen, L. Huang, L. Zhang, H. Pan, B. Wu, and Y. Lin, *Sci. Rep.* 5, 10460 (2015).
4. P. Pust, V. Weiler, C. Hecht, A. Tücks, A.S. Wochnik, A.K. Henß, D. Wiechert, and C. Scheu, *Nat. Mater.* 13, 891 (2014).
5. H.P.T. Nguyen, Q. Wang, and Z. Mi, *J. Electron. Mater.* 43, 868 (2014).
6. H. Pan, L. Zhang, L. Jin, B.B. Zhang, and W.Q. Yang, *J. Electron. Mater.* 44, 3465 (2015).

7. B. Wu, W.Q. Yang, H.G. Liu, H. Li, B.W. Zhao, C. Wang, G.L. Xu, and Y. Lin, *Spectrochim. Acta Part A* 123, 12 (2014).
8. J.K. Park, M.A. Lim, C.H. Kim, H.D. Park, J.T. Park, and S.Y. Choi, *Appl. Phys. Lett.* 82, 683 (2003).
9. Q. Li, L. Gao, and D. Yan, *Mater. Chem. Phys.* 64, 41 (2000).
10. F. Wang, D. Zhou, S. Ma, H. Yu, P. Li, and Z. Yang, *J. Alloys Compd.* 509, 4824 (2011).
11. H.J. Yu, W. Chung, H. Jung, S.H. Park, J. Kim, and S.H. Kim, *Mater. Lett.* 65, 2690 (2011).
12. S.X. Yan, J.H. Zhang, X. Zhang, S. Lu, X. Ren, Z. Nie, and X. Wang, *J. Phys. Chem. C* 111, 13256 (2007).
13. C. Guo, D. Huang, and Q. Su, *Mater. Sci. Eng. B* 130, 189 (2006).
14. F. Yang, Z. Yang, Q. Yu, Y. Liu, X. Li, and F. Lu, *Spectrochim. Acta A* 105, 626 (2013).
15. R. Fujiwara, H. Sano, M. Shimizu, and M. Kuwabara, *J. Lumin.* 129, 231 (2009).
16. F.J. Chun, B.B. Zhang, H. Su, H. Osman, W. Deng, W.L. Deng, H.T. Zhang, X.Y. Zhao, and W.Q. Yang, *J. Lumin.* 190, 69 (2017).
17. W. Tang, Y. Sun, M. Yu, X. Liu, Y.Q. Yin, B. Yang, L.M. Zheng, F. Qin, Z.G. Zhang, and W.W. Cao, *RSC Adv.* 5, 27491 (2015).
18. L. Zhang, H. Pan, H.G. Liu, B. Zhang, L. Jin, M.H. Zhu, and W.Q. Yang, *J. Alloys Compd.* 643, 247 (2015).
19. W. Ran, L. Wang, H. Li, Y. Guo, W. Kang, D. Qu, J. Shi, and L. Su, *Ceram. Int.* 41, 4301 (2015).
20. Z. Li, Y. Wang, J. Cao, Y. Jiang, X. Zhao, Z. Meng, and J. Rare, *Earths* 34, 143 (2015).
21. C.S. Wu, B.T. Sen, and M.D. Jean, *J. Electron. Mater.* 43, 465 (2014).
22. G. Ramakrishna, H. Nagabhushana, S.C. Prashantha, S.C. Sharma, and B.M. Nagabhushana, *Spectrochim. Acta A* 136, 356 (2015).
23. J.K. Han, M.E. Hannah, A. Piquette, J.B. Talbot, K.C. Mishra, and J. McKittrick, *J. Lumin.* 16, 20 (2015).
24. Y.W. Liu, Q. Fang, L.X. Ning, Y.C. Huang, S.Z. Huang, and H.B. Liang, *Opt. Mater.* 44, 67 (2015).
25. J. Barzowska, K. Szczodrowski, M. Krośnicki, B. Kuklińs-ki, and M. Grinberg, *Opt. Mater.* 34, 2095 (2012).
26. H. Yu, Y.W. Lai, G.M. Gao, L. Kong, G.H. Li, S.C. Gan, and G.Y. Hong, *J. Alloys Compd.* 509, 6635 (2011).
27. X.L. Liu, Y.Y. Fan, S.W. Chen, M. Gu, C. Ni, B. Liu, and S.M. Huang, *Mater. Res. Bull.* 48, 2370 (2013).
28. R.P. Cao, Q.Q. Xiong, W.J. Luo, D.L. Wu, F. Xiao, and X.G. Yu, *Ceram. Int.* 41, 7191 (2015).
29. H. Yu, G.M. Gao, L. Kong, G.H. Li, S.C. Gan, G.Y. Hong, and J. Rare, *Earths* 29, 431 (2011).
30. W. Luo, D. Tu, R. Li, X. Mao, Y. Xu, J. Ren, B. Li, and H. Wu, *J. Mater. Sci.* 52, 9764 (2017).
31. L. Kong, X. Xiao, J. Yu, D. Mao, and G. Lu, *J. Mater. Sci.* 52, 6310 (2017).
32. W.Q. Yang, W.C. Zheng, and H.G. Liu, *Spectrochim. Acta A* 78, 231 (2011).
33. H. Liu, D. Xu, Q. Xu, Q. Di, and J. Sun, *J. Mater. Sci.* 50, 2257 (2015).
34. H. Yu, X. Yu, X. Xu, T. Jiang, and P. Yang, *Opt. Commun.* 317, 78 (2014).
35. B. Bondzior, D. Stefańska, A. Kubiak, and P.J. Dereń, *J. Lumin.* 173, 38 (2016).
36. M. Sobczyk, D. Szymański, M. Guzik, and J. Legendzie-wicz, *J. Lumin.* 166, 40 (2015).
37. R. Zhou, L. Wang, M. Xu, and D. Jia, *J. Alloys Compd.* 647, 136 (2015).
38. Z. Wang, P. Li, Z. Yang, and Q. Guo, *J. Lumin.* 132, 1944 (2012).
39. R.J. Wiglusz, T. Grzyb, A. Lukowiak, A. Bednarkiewicz, S. Lis, and W. Strek, *J. Lumin.* 133, 102 (2013).
40. L. Cheng, W.T. Zhang, Y.H. Li, S.Y. Dai, X.F. Chen, and K.H. Qiu, *Ceram. Int.* 43, 11244 (2017).
41. Z.J. Wang, S.Q. Lou, and P.L. Li, *J. Alloys Compd.* 658, 813 (2016).
42. C. Tanaka, Y. Yokota, S. Kurosawa, A. Yamaji, Y. Ohashi, K. Kamada, M. Nikl, and A. Yoshikawa, *J. Cryst. Growth* 468, 399 (2017).
43. R.J. Wiglusz, T. Grzyb, A. Lukowiak, P. Gluchowski, S. Lis, and W. Strek, *Opt. Mater.* 35, 130 (2012).